



A publication of the
**American
Pharmaceutical
Association**
and the
**American
Chemical
Society**



JOURNAL OF Pharmaceutical Sciences

April 1999

Volume 88, Number 4

Characterization of Tolbutamide Polymorphs (Burger's Forms II and IV) and Polymorphic Transition Behavior

KENYA KIMURA, FUMITOSHI HIRAYAMA, AND KANETO UEKAMA*

Contribution from *The Faculty of Pharmaceutical Sciences, Kumamoto University, 5-1 Oe-honmachi, Kumamoto 862-0973, Japan.*

Received September 17, 1998. Accepted for publication January 20, 1999.

Abstract □ Burger's two polymorphs of tolbutamide (TB), an oral hypoglycemic agent, were obtained by spray-drying the drug dissolved in a mixed solvent of ethanol/dichloromethane (Form IV) and allowing Form IV to stand at constant temperatures and humidities (Form II). These polymorphs were characterized by various physical methods [e.g., powder X-ray diffractometry, differential scanning calorimetry, infrared spectrometry, and solid-state carbon-13 nuclear magnetic resonance (^{13}C NMR) spectroscopy] and compared with two other TB polymorphs Forms I and III. The ^{13}C NMR spectra showed that the chemical shift and the peak shape of resonance associated with the toluene and *n*-butyl moieties of TB were different for each of the four polymorphs, whereas the carbonyl carbon was unchanged, indicating different conformations and molecular motions of the toluene and *n*-butyl moieties in the solid states. Form IV converted itself to Form II within 3 h when it was stored at 45 °C and 75% relative humidity (RH) and, in turn, Form II transformed to Form I at higher temperatures. The conversion of Form IV to Form II proceeded according to a zero-order equation (Polanyi–Winger equation), and that of Form II to Form I according to a first-order equation. The increase in RH accelerated the polymorphic transition of Form IV. Both the apparent dissolution rate and the solubility of Form IV were nearly identical with those of Form II, because the former changed to the latter during the dissolution, but their dissolution rates and solubility were higher than those of Forms I and III. These dissolution characteristics of TB polymorphs were reflected in the oral absorption behavior in dogs; that is, the bioavailability increased in the order Form I < Form III < Form II \approx Form IV.

Introduction

Pharmaceutical solids can exist in different crystal forms, such as crystalline, amorphous, or glass, and also in

solvated or hydrated states.^{1–3} Because of the difference in molecular packing, polymorphic forms of solid drugs influence their dissolution rate, solubility, stability, bioavailability, pharmaceutical manufacturing, etc.^{4–6} Therefore, some of the most important components of pharmaceutical solid formulation are the detection of as many polymorphs as possible, as well as their characterizations and selection of the desired ones. Tolbutamide [1-butyl-3-{4-methylphenylsulfonyl}urea, TB] is an oral hypoglycemic agent used clinically in the treatment of insulin-dependent diabetic patients.⁷ Early studies have suggested that TB has several polymorphs in the solid states.^{8–17} For example, Simmons et al.⁸ reported the presence of two polymorphs, whereas Burger et al.⁹ and Traue et al.¹⁴ suggested the existence of four polymorphs. The Simmons's Forms A and B are identical with the Burger's Form I and III, respectively, and have been well characterized. However, Burger's Forms II and IV have been not fully characterized; for example, the diffraction pattern of the Georgarakis's Form II is different from that of the Al-Saieq's Form II but resembles that of Form IV.^{11,15} In this study, two polymorphs (Forms II and IV) of TB were prepared and characterized by various physical methods [e.g., powder X-ray diffractometry (PXRD), differential scanning calorimetry (DSC), infrared (IR) spectrometry, and solid-state carbon-13 nuclear magnetic resonance (^{13}C NMR) spectroscopy] and compared with the TB polymorphs Forms I and III reported by Simmons et al.⁸ Furthermore, the polymorphic transition behavior of Form IV was investigated. Because TB is a poorly water-soluble drug with several different polymorphs, its tablets are obligated to pass the dissolution test in Japanese Pharmacopoeia.¹⁸ The dissolution and in vivo absorption behavior of Form IV in dogs were compared with those of Forms I, II, and III.

* To whom correspondence should be addressed. Telephone and fax: (+81-96)-371-4160. E-mail: uekama@gpo.kumamoto-u.ac.jp.

Experimental Section

Materials—TB (purity > 99%) and chlorpropamide were donated by Nippon Hoechst-Marion-Roussel Ltd. (Tokyo, Japan) and Ono Pharmaceutical Company (Osaka, Japan), respectively. Other chemicals and solvents were of analytical reagent grade, and deionized double-distilled water was used throughout the study.

Apparatus—The PXRD patterns were measured with a Rigaku Rint-2500 diffractometer (Tokyo, Japan) under the following conditions: Ni-filtered Cu-K α radiation (1.542 Å), a voltage of 40 kV, a current of 40 mA, a divergent slit of 1.74 mm (1°), a scattering slit of 0.94 mm (1°), a receiving slit of 0.15 mm, and a goniometer angular increment of 1°/min. The theoretical diffraction profiles on the basis of single-crystal X-ray analysis data were drawn using the teXsan crystallographic software package of Molecular Structure Corporation¹⁹ on a Silicone Graphics IRIS Indigo work station (U.S.A.). The DSC analyses were carried out using a Perkin-Elmer DSC-7 thermal analyzer (Norwalk, CT) with a data analysis system (DEC station 325C computer, U.S.A.), operated with sample weights of 5 mg and a scanning rate of 10 °C/min. The heat fusion was calibrated with indium (purity, 99.999%; melting point, 156.4 °C; ΔH 28.47 mJ/mg; heating rate, 10 °C/min). Fourier transform infrared (FT-IR) spectra were recorded using a JEOL JIR-6500 FT-IR spectrometer (Tokyo, Japan) on samples prepared with KBr. The solid-state ¹³C NMR spectra were taken on a JEOL JNM EX-270 spectrometer with a cross polarization/magic angle spinning (CP/MAS) accessory (Tokyo, Japan). The operating conditions were 270 MHz (¹H) and 25 °C. The CP radio frequency field strength was about 56 kHz, the contact time was 5 ms and the MAS rate was 6 kHz. The ¹³C NMR chemical shifts were measured with respect to the resonance of tetramethylbenzene (17.3 ppm downfield from the resonance of tetramethylsilane). The chemical shift of TB was assigned according to the report of Ueda et al.²⁰ Crystal appearance was observed with a scanning electron microscope (SEM) instrument (Hitachi-Akashi S-501, Tokyo, Japan), after crystals were mounted onto an SEM sample stub with double-sided sticky tape and coated with gold by a direct current sputter technique.

Preparation of TB Polymorphs—Form I of TB was prepared according to the method of Simmons;⁸ that is, TB (5 g) was dissolved in benzene (10 mL) at 70 °C, and then hexane (5 mL) was slowly added. The resulting solution was allowed to stand at room temperature. Form III was prepared by dissolving TB (5 g) in ethanol (10 mL) at 60 °C, slowly adding warm water, and allowing the resulting solution to stand at room temperature.⁸ Form II was prepared by storing Form IV at 60 °C, 75% RH for 10 min. Form IV was prepared by the spray-drying method; that is, TB was dissolved in the mixed solvent ethanol/dichloromethane (1.2:1 v/v, 150 mL) and subjected to spray-drying, using a Pulvis GA32 Yamato spray-drier (Tokyo, Japan) under the following conditions: an air flow rate of 0.4 m³/min, an air pressure of 1.0 kgf/cm², and inlet and outlet temperatures of 85 and 55 °C, respectively.

Aging Studies—The test powder (about 300 mg, <100 mesh) was placed in glass containers in desiccators at constant humidity (saturated solutions of potassium acetate, sodium bromide dihydrate, and sodium chloride at 22%, 50% and 75% RH, respectively), and then stored in incubators at constant temperatures (35–70 °C).^{21,22} The phase change of TB crystals was monitored by PXRD.

Dissolution Studies—The dissolution rate of TB polymorphs was measured according to the dispersed amount method.²³ A fixed amount (100 mg, <100 mesh) of TB polymorphs was put into 25 mL of Japanese Pharmacopoeia XIII (JP XIII) second fluid (pH 6.8) and stirred at 91 rpm at 37 °C. At appropriate intervals, an aliquot (1.0 mL) was withdrawn with a cotton plugged pipet and analyzed for TB spectrophotometrically at 230 nm. To monitor the polymorphic change of TB during the dissolution, DSC curves were made of the powder suspended in the medium after drying under reduced pressure for 1 day.

Absorption Studies—The absorption studies were carried out using male beagle dogs (9–11 kg) that were fasted for 24 h before drug administration. The sample (equivalent to 100 mg/body) was wrapped in a wafer and administered orally with water (50 mL), using a catheter. Blood samples (1 mL) were withdrawn from the cephalic vein with a heparinized injection syringe and centrifuged at 1100 $\times g$ for 10 min. The plasma (0.2 mL) was added to the solution containing an internal standard, chlorpropamide (1.0 mg/mL, 0.5 mL), and extracted with ethyl ether (4.0 mL). The organic

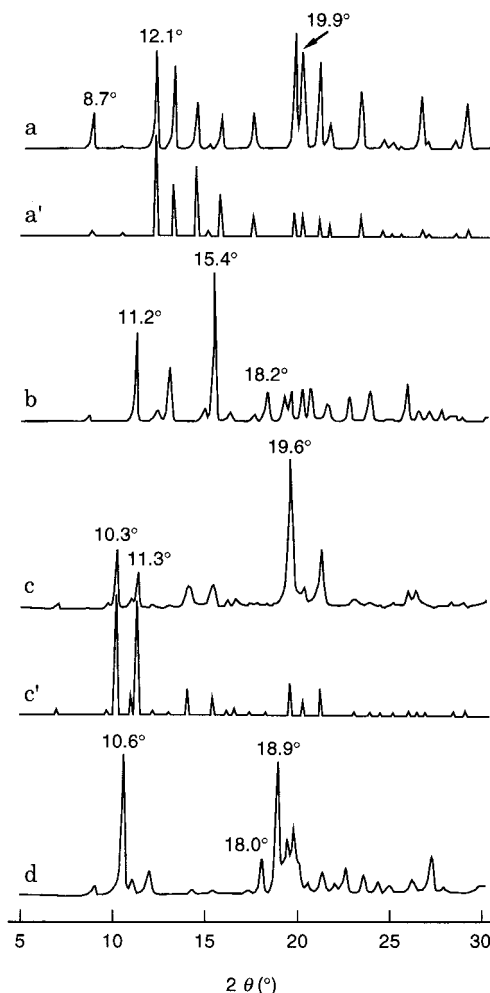


Figure 1—PXRD patterns of TB polymorphs: (a) Form I; (a') theoretical profile of Form I; (b) Form III; (c) Form II; (c') theoretical profile of Form II; (d) Form IV.

phase (3.0 mL) was evaporated, the residue was dissolved in acetonitrile (0.1 mL), and TB was determined by high-performance liquid chromatography (HPLC) with an Hitachi L-600 pump and a 635A UV detector (Tokyo, Japan), a Yamamura YMC AQ-312 ODS column (5 μ m, 6 \times 150 mm, Kyoto, Japan), a mobile phase of acetonitrile/0.05 M NaH₂PO₄ solution (45:55 v/v), a flow rate of 1.6 mL/min, and detection at 230 nm.

Results and Discussion

Characterization of TB Polymorphs—Figure 1 shows PXRD patterns of the TB solids (Forms I, II, III, and IV). Form IV was prepared by spray-drying TB using the mixed solvent ethanol/dichloromethane (1.2:1 v/v) and Form II was prepared by storing Form IV at 60 °C, 75% RH (see *Experimental Section*). Form I of TB gave diffraction peaks at 8.7, 12.1, and 19.9°, and this pattern coincided in diffraction angle and with the computer-simulated pattern drawn on the basis of single-crystal data of Form I reported by Donaldson et al.²⁴ The difference in diffraction intensity at $2\theta =$ about 20° may be ascribed to the difference in crystal habit of the two samples. Rowe and Anderson reported that Form III is less soluble than Form I in water at 37 °C; thus, Form III is a stable form at room temperature, although the difference in free energy of the two forms is small.²⁵ Form III gave diffraction peaks at 11.2, 15.4, and 18.2° and Form II at 10.3, 11.3 and 19.6°. The diffraction pattern of Form II was identical in diffraction angle to the computer-simulated pattern drawn on the

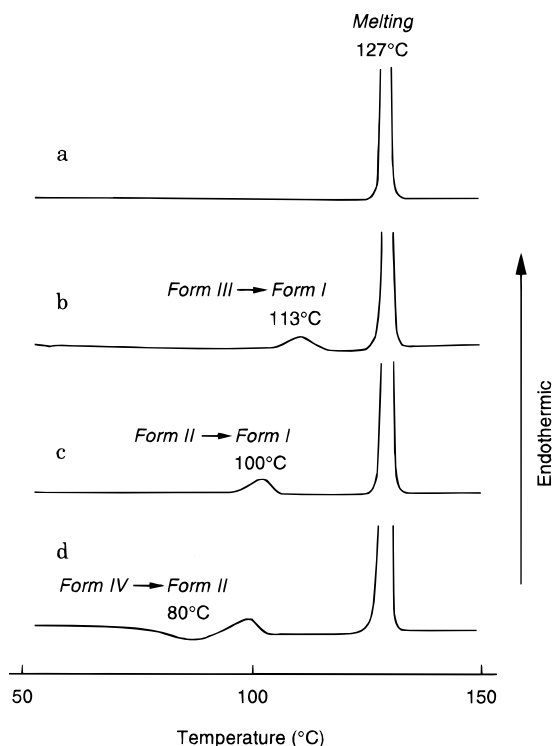


Figure 2—DSC thermograms of TB polymorphs: (a) Form I; (b) Form III; (c) Form II; (d) Form IV.

basis of single-crystal data of Form II, which was analyzed in our laboratory and will be reported elsewhere.²⁶ The difference in diffraction intensity may be also ascribed to the difference in crystal habit of the two samples. On the other hand, the spray-dried TB gave two strong diffraction peaks at 10.6 and 18.9° and a small peak at 18.0°, which were clearly different from those of Forms I, II, and III, although its diffraction pattern resembled that of Form II. These results suggest that the spray-dried TB is one of polymorphs of TB and its internal structure may resemble that of Form II. These polymorphs of TB, Forms II and IV, were further characterized by other physical methods.

Figure 2 shows DSC curves of Forms I, II, III, and IV. Form I showed an endothermic peak at 127 °C due to melting. Form III gave two peaks at 113 and 127 °C. The latter peak is due to the melting of Form I and the former peak is due to the melting of Form III followed by the crystallization of Form I, because the PXRD pattern of Form III heated to about 110 °C coincided with that of Form I. Form II showed a similar polymorphic transition behavior; that is, the melting of Form II and crystallization of Form I at 100 °C and the melting of Form I at 127 °C. On the other hand, Form IV showed an exothermic peak at 80 °C, followed by endothermic peaks at 100 and 127 °C. The PXRD pattern of Form IV heated to 80 °C was identical to that of Form II, indicating that the 80 °C peak is due to the transition of Form IV to Form II, the 100 °C peak is due to the melting of Form II and crystallization of Form I, and the 127 °C peak is due to the melting of Form I. The conversion of Form IV to Form II was apparently accompanied by no liquification, whereas that of Form II to Form I is a crystallization from the liquified Form II. The enthalpy changes (ΔH) for the conversion of Form IV to Form II and the melting of Form I were 1.2 and 27.2 kJ/mol, respectively. The apparent ΔH values for the conversion of Forms III and II to Form I were 1.9 and 1.5 kJ/mol, respectively, although they contain the combined ΔH changes of fusion and crystallization processes.

Figure 3 shows SEM pictures of the four TB polymorphs.

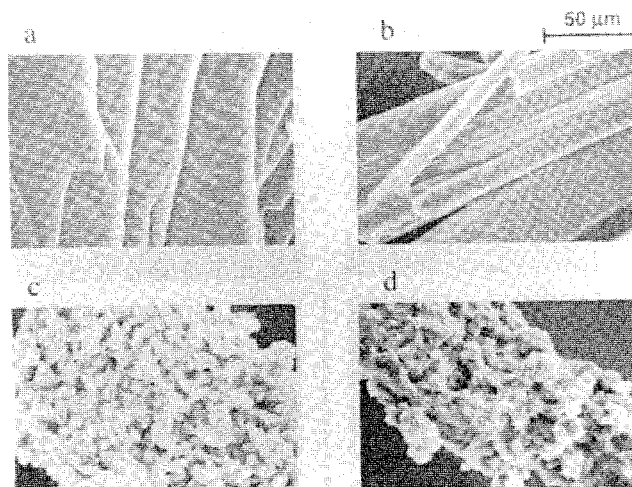


Figure 3—Scanning electron micrographs of TB polymorphs: (a) Form I; (b) Form III; (c) Form II; (d) Form IV.

Form I is in the form of plate crystals with a microscopically layered sheet structure and Form III consists of needlelike crystals, with both forms having smooth surfaces. Form II, an aggregate, consists of small solid particles, whereas Form IV has a rodlike structure, with many pores and clusters of small particles on the surface, and its appearance resembles that of Form II.

The solid-state ¹³C NMR spectroscopic studies were employed to gain insight into the internal structure of TB polymorphs. Figure 4 shows ¹³C NMR spectra of Forms I, II, III, and IV measured in a CP/MAS mode. The chemical shifts are listed in Table 1. These ¹³C NMR signals were assigned according to the spectrum of TB in solution.²⁰ In Form I, the butyl and methyl carbons gave sharp peaks, suggesting a definite conformation²⁴ as described later, whereas the benzene carbons gave rather broad peaks with a shoulder, suggesting that each *ortho*- and *meta*-carbon is magnetically nonequivalent and the broadening of the C2 carbon may arise from a magnetic fluctuation due to a rotation of the methyl group. Form III gave chemical shifts similar to those of Form I, although the signals of the *ortho*- (C4 and C6) and *meta*- (C3 and C7) carbons became sharp whereas those of the C10–C12 carbons split. These results suggest that the conformation of TB in Form III is very similar to that in Form I, but with different motional freedom as reflected by the observed NMR peak splitting. On the other hand, the chemical shifts of the butyl moiety in Forms II and IV were significantly different from those in Forms I and III, although the benzene ring had similar chemical shifts; that is, C10 carbon: 31.8 ppm (Form I), 30.9 and 31.9 ppm (Form III), 35.2 and 33.4 ppm (Form II), and 33.8 ppm (Form IV); C12 carbon: 13.6 ppm (Form I), 12.7 and 12.0 ppm (Form III), 15.8 and 13.7 ppm (Form II), and 16.1 ppm (Form IV). Our results on the single-crystal analysis of Form II²⁶ and the reported result of Form I²⁴ indicate that the butyl moiety of TB is in a *trans* conformation in Form II crystals (C9–C10–C11–C12 dihedral angle = 178.6°) but it is in a *gauche* conformation in Form I crystals (the dihedral angle = 101.3°). Therefore, the shift difference of the butyl moiety can be ascribed to this conformational alteration. The chemical shifts of TB in Form IV were very similar to those in Form II, although the signals of the *ortho*- and *meta*-carbons became sharp. These results indicate that the conformation of TB in Form IV is almost the same as that of Form II, but the environment around the benzene ring may differ; that is, there may be some vacant space that allows the ring to rotate due to the looser packing of crystals in Form IV. The FT-IR spectroscopic studies supported this conclusion; that

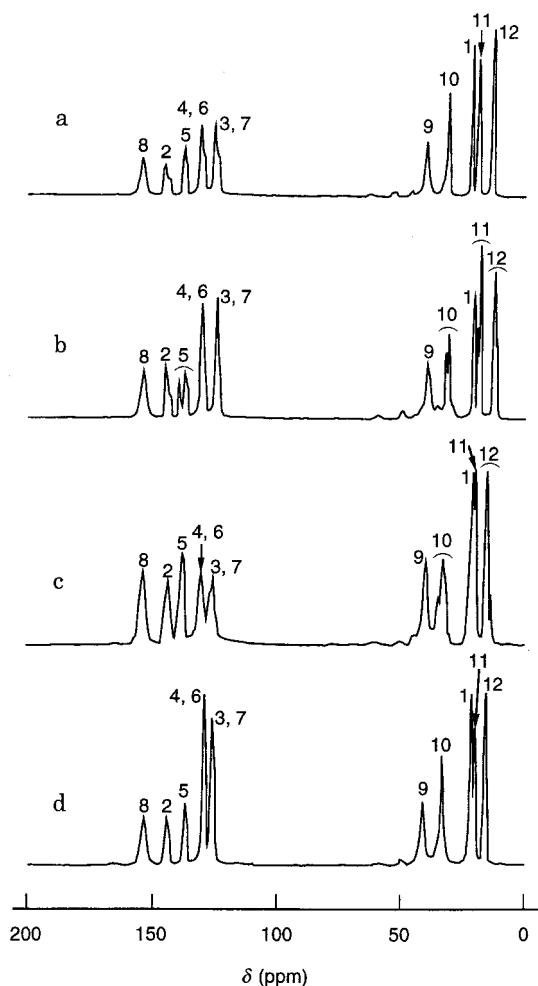
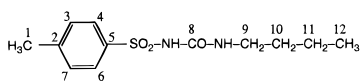


Figure 4— ^{13}C CP/MAS NMR spectra of TB polymorphs at 25 °C (see Table 1 for the carbon numbering of TB): (a) Form I; (b) Form III; (c) Form II; (d) Form IV.

Table 1— ^{13}C NMR Chemical Shifts (ppm)^a of TB Polymorphs at 25 °C



carbon	solution		solid state			
	in 2 N NaOD	Form I	Form III	Form II	Form IV	
1	21.6	21.8	20.9	21.7	22.1	
2	144.9	145.8	145.1	144.2	144.8	
3, 7	127.0	126.2	125.0	126.2	127.2	
4, 6	130.1	131.8	131.0	130.9	130.4	
5	136.7	138.1	139.8, 137.4	138.6	137.5	
8	151.3	155.0	154.1	154.3	154.0	
9	40.2	40.1	39.2	40.2	41.5	
10	31.6	31.8	31.9, 30.9	35.2, 33.4	33.8	
11	19.9	19.4	19.5, 18.6	20.6	20.7	
12	13.7	13.6	12.7, 12.0	15.8, 13.7	16.1	

^a Downfield from the resonance of tetramethylsilane.

is IR absorption bands of the functional groups involving in the intermolecular hydrogen bonding of TB molecules, such as the imino (NH, 3328 cm^{-1}), carbonyl (CO, 1703 and 1660 cm^{-1}), and sulfonyl (SO_2 , 1336 and 1159 cm^{-1}) groups, showed insignificant differences in the wavelength between the four TB polymorphs, suggesting the similar hydrogen bonding network.^{24,26} On the other hand, the spectral shapes of the stretching absorption band of alkyl portion around 2950–3000 cm^{-1} and the aromatic CH stretching

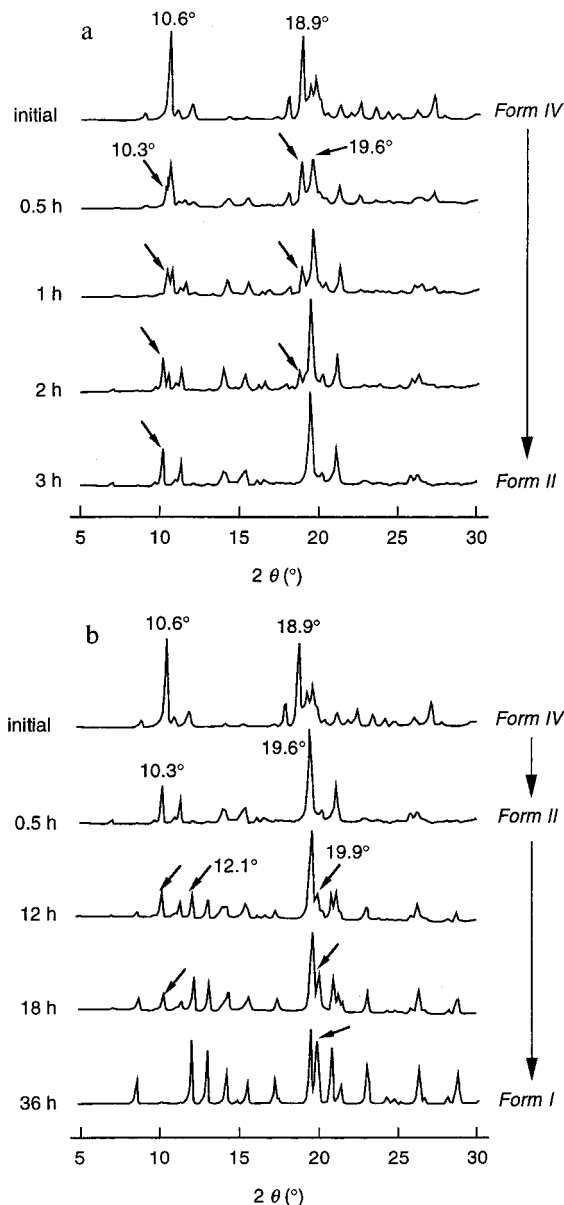


Figure 5—Changes of PXRD pattern of Form IV during storage at (a) 45 °C and 75% RH and (b) 60 °C and 75% RH.

band around 800–850 cm^{-1} were different between the four polymorphs. As judged by the peak intensities of 816 and 843 cm^{-1} , our Forms I, II, III, and IV are identical with Burger's Forms I, II, III, and IV, although it is difficult to completely identify the latter because no diffraction data are given in his paper.⁹ However, it is apparent from the diffraction data, that Al-Saieq's¹¹ Form IV corresponds to our Form II and Georgarakis's¹⁵ Form II corresponds to our Form IV.

Transition Behavior of Form IV—The isothermal transition behavior of Form IV was investigated because it may be easily converted to Form II, which has a similar crystal structure. Figure 5 shows changes in the PXRD pattern of Form IV during storage at 45 and 60 °C at 75% RH. During the storage at 45 °C (Figure 5a), the diffraction peaks characteristic of Form IV at $2\theta = 10.6^\circ$ and 18.9° decreased, whereas those of Form II at 10.3° and 19.6° increased. The longer storage at the higher temperature (Figure 5b) gave diffraction peaks characteristic of Form I at 12.1° and 19.9° , indicating the transition of Form IV to Form I via Form II. Figure 6 shows the time courses for the conversion of Form IV to Forms II and I on storage at

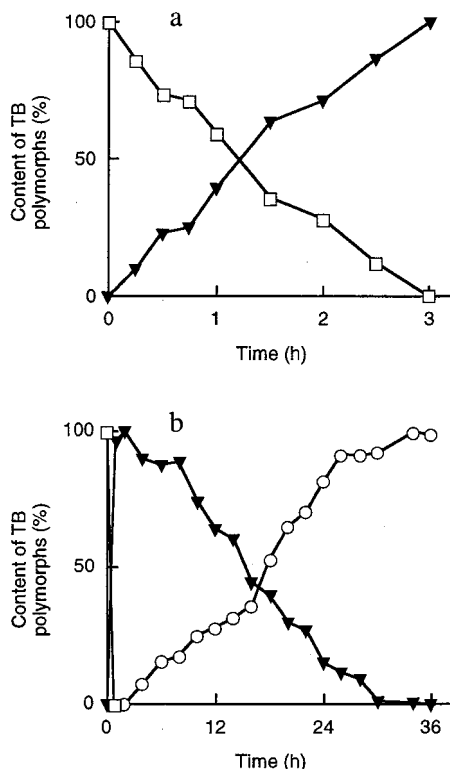


Figure 6—Time courses for conversion of Form IV to Form II and Form I during storage at (a) 45 °C and 75% RH and (b) 60 °C and 75% RH. Key: (○) Form I; (▼) Form II; (□) Form IV.

the conditions just stated. The contents of each polymorph were determined from the following diffraction intensity ($2\theta = 19.9^\circ$ for Form I, 10.3° for Form II, and 18.9° for Form IV). Form IV was converted completely to Form II in 3 h with storage at 45 °C, 75% RH, whereas at 60 °C, Form IV rapidly changed to Form II within 30 min and Form II slowly changed to Form I in 30 h. These polymorphic transition-time profiles were analyzed according to the Hancock and Sharp equation (eq 1):²⁷

$$\ln[-\ln(1 - \alpha)] = m \ln t + \ln B \quad (1)$$

where m is the intrinsic value for various theoretical equations of solid-state decomposition, α is the fraction of the total sample converted to the other polymorph, based on the X-ray relative intensities, t is the storage time, and B is a constant. The plot of $\ln[-\ln(1 - \alpha)]$ versus $\ln t$ using the data of $\alpha = 0.1-0.5$ gave straight lines of $m = 1.23 \pm 0.06$ (mean \pm SE, $n = 4$, correlation coefficient (r) = 0.998) for the conversion of Form IV to Form II at 45 °C and 75% RH, and $m = 0.99 \pm 0.04$ ($n = 4$, $r = 0.997$) for that of Form II to Form I at 60 °C and 75% RH. The m value of 1.23 indicates that the Form IV-to-II transition proceeds according to a zero-order mechanism (a criterion for zero-order transition: $m = 1.24$)²⁷ and its rate obeys the equation of $\alpha = kt$. On the other hand, the m value of 0.99 indicates that a random nucleation on each particle is a rate-determining step for the Form II-to-Form I transition (a criterion for this conversion is $m = 1.0$)²⁷ and its rate obeys the equation of $-\ln(1 - \alpha) = kt$. Therefore, the polymorphic transition rates of Form IV to Form II and Form II to Form I were analyzed, respectively according to the aforementioned equations, and the results at various temperatures are shown in Figure 7. The plots of α or $-\ln(1 - \alpha)$ versus t were confirmed to be linear, and the transition rate constants (k , see Figure 7) were obtained from the slopes. The Arrhenius plots of these rate constants gave straight lines ($r = 0.999$), from which the activation

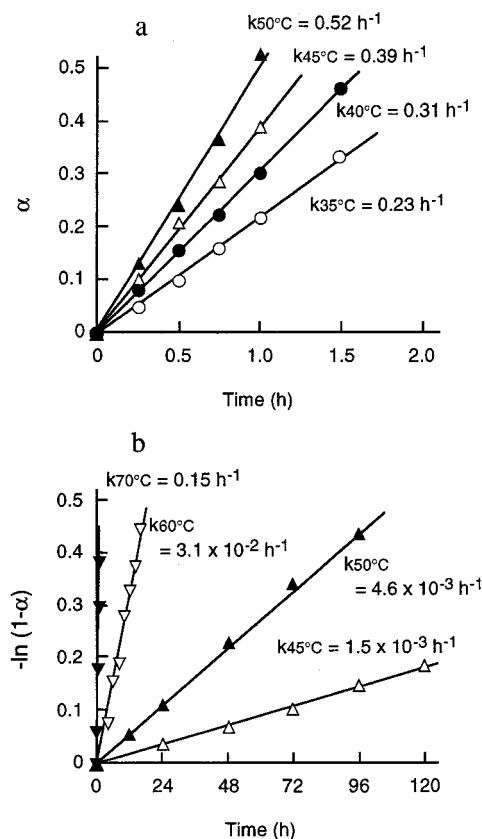


Figure 7—Plots of α and $-\ln(1 - \alpha)$ for transitions of (a) Form IV to Form II and (b) Form II to Form I at 75% RH. Key: (○) 35 °C; (●) 40 °C; (△) 45 °C; (▲) 50 °C; (▽) 60 °C; (▼) 70 °C.

energies of 44 and 166 kJ/mol were obtained for the transitions of Form IV to II and Form II to I, respectively. These results indicate that the energy barrier of the transition of Form IV to Form II is very low, because the internal structure of Form IV, including the conformation of TB, is similar to that of Form II, whereas that of Form II to Form I is rather high because the crystal system and the conformation of TB are different between Form II (monoclinic, $P2_1/n$, $a = 11.815 \text{ \AA}$, $b = 9.069 \text{ \AA}$, $c = 13.981 \text{ \AA}$, $\beta = 104.50^\circ$)²⁶ and Form I (orthorhombic, $Pna2_1$, $a = 20.223 \text{ \AA}$, $b = 7.831 \text{ \AA}$, $c = 9.090 \text{ \AA}$)²⁴ crystals. The transition behavior of Form IV at different humidity conditions (22, 50, and 75% RH) and 50 and 60 °C was investigated, and the rate constants were obtained from the linear plots of α and $-\ln(1 - \alpha)$ versus t for the Form IV-to-Form II transition and the Form II-to-Form I transition, respectively, as follows: $k = 0.16, 0.52$, and 1.01 h^{-1} for the Form IV-to-Form II transition at 50 °C, and $k = 0.0030, 0.012$, and 0.031 h^{-1} for the Form II-to-Form I transition at 60 °C. The transition rate increased as the humidity increased, presumably because TB dissolves in adsorbed water on the crystal surface, which may consequently promote the nucleation and growth of crystals.

Dissolution and Absorption Behavior of Polymorphs—Figure 8 shows dissolution profiles of TB polymorphs in the JP XIII second fluid (pH 6.8), measured by the dispersed amount method at 37 °C. The dissolution rate of Form III was slightly faster than that of Form I, whereas those of Forms IV and II were significantly faster than that of Form I. The dissolution rate of Form IV was almost the same as that of Form II. The Form IV powder in the dissolution medium was taken out, dried, and subjected to DSC measurements to gain insight into phase changes of Form IV during the dissolution. As is apparent from the change in DSC curves in Figure 9, Form IV transformed

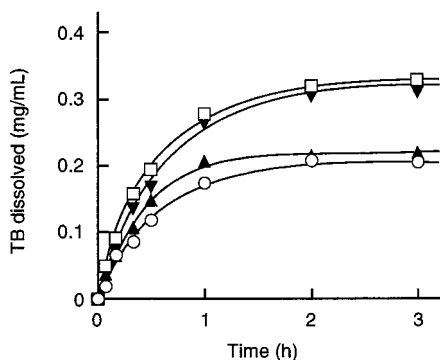


Figure 8—Dissolution profiles of TB polymorphs (equivalent to 100 mg TB) in JP XIII second fluid at 37 °C, measured by the dispersed amount method at 91 rpm. Key: (○) Form I; (▲) Form III; (▼) Form II; (□) Form IV. Each point represents the mean of 3 experiments.

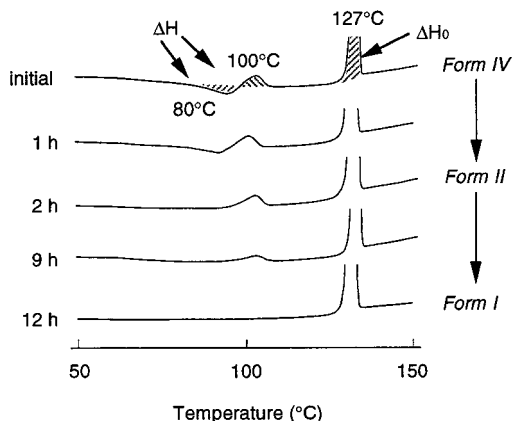


Figure 9—DSC thermograms of Form IV during dissolution in JP XIII second fluid at 37 °C, measured by the dispersed amount method at 91 rpm.

into Form I via Form II during the dissolution. The apparent first-order transition rate constants of Form IV to Form II and Form II to Form I under the dissolution test condition (dispersed amount method, JP XIII second fluid, powder size < 100 mesh, 37 °C, 91 rpm) were determined by plotting the data of $\ln(\Delta H/\Delta H_0)$ versus time, where ΔH_0 is the enthalpy change for fusion of total Form I at 127 °C. The enthalpy changes (ΔH) of the exothermic peak at about 80 °C during 0–2 h were used for calculation of the rate constant of the Form IV-to-Form II transition, and those of the adjacent endothermic peak (about 100 °C) after 2 h were used for the rate constant calculation of the Form II-to-Form I transition. The first-order plot of both transitions gave a straight line ($r = 0.998$), from which the rate constants of 0.45 and 0.087 h^{-1} for the transitions of Form IV to Form II and Form II to Form I, respectively, were obtained. Therefore, the insignificant difference in the dissolution rate between Forms IV and II can be attributed to the phase change of Form IV to Form II within about 2 h under experimental conditions. Figure 10 shows the plasma TB level–time profiles after oral administration of TB polymorphs in dogs. Their bioavailability parameters are summarized in Table 2. The oral bioavailability of TB increased in the order Form I \ll Form III $<$ Form II \approx Form IV, and that of Forms IV and II was >2-fold higher than that of Form I, reflecting the in vitro dissolution behavior of the polymorphs.

Conclusion

In this study, we fully characterized polymorphs of TB (Burger's Forms I, II, III, and IV) by various physical

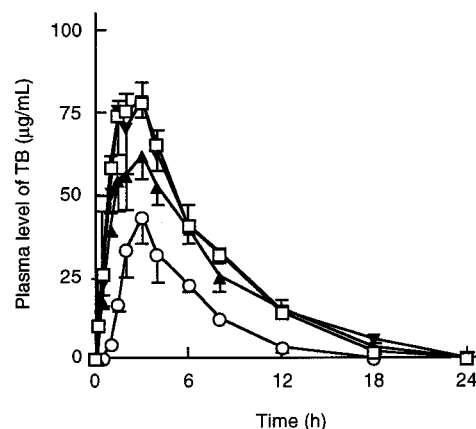


Figure 10—Plasma levels of TB after oral administration of TB polymorphs (equivalent to 100 mg/body TB) in dogs. Key: (○) Form I; (▲) Form III; (▼) Form II; (□) Form IV.

Table 2—Bioavailability Parameters of TB after Oral Administration of TB Polymorphs (Equivalent to 100 mg/body TB) in Dogs^a

Form	t_{\max} (h) ^b	C_{\max} ($\mu\text{g/mL}$) ^c	AUC ($\text{h}\cdot\mu\text{g/mL}$) ^d	MRT (h) ^e	F (%) ^f
I	3.0 \pm 0.0	43.6 \pm 7.1	226.1 \pm 34.6	5.1 \pm 0.1	19.2 \pm 3.6
III	2.7 \pm 0.3	62.1 \pm 6.1	489.0 \pm 64.7**	6.1 \pm 0.3**	41.6 \pm 6.7**
II	2.2 \pm 0.4	84.8 \pm 9.3*	590.0 \pm 74.7**	6.0 \pm 0.3**	50.2 \pm 7.8**
IV	2.7 \pm 0.3	80.5 \pm 2.8**	576.0 \pm 33.6*	5.5 \pm 0.2	49.0 \pm 3.5**

^a Each value represents the mean \pm SE of 3 dogs; significant difference from Form I is noted as follows: (*) $p < 0.05$; (**) $p < 0.01$. ^b The time required to reach the maximum plasma level. ^c The maximum plasma level. ^d The area under the plasma level versus time curve up to 24 h post-administration. ^e The mean residence time in plasma. ^f The extent of bioavailability compared with the AUC value of intravenously administered TB.

methods such as XRPD, solid-state ^{13}C NMR, FT-IR, and thermal analysis. The results indicate that Form IV has an internal structure and conformation that resemble closely those of Form II. Because of this similarity, Form IV was easily converted to Form II under both isothermal and nonisothermal conditions. The dissolution rate of Form IV was almost identical to that of Form II because of the conversion to Form II during the dissolution. This dissolution property of Form IV was clearly reflected in the oral bioavailability of TB in dogs. The present systematic characterization of TB polymorphs will be useful for identification of solid TB and gives a rational basis for the design of solid TB formulations.

Supporting Information Available— Four figures of TB polymorphs (FT-IR spectra and conversion plots). This material is available free of charge via the Internet at <http://pubs.acs.org>.

References and Notes

- Haleblian, J.; McCrone, W. Pharmaceutical applications of polymorphism. *J. Pharm. Sci.* **1969**, *58*, 911–929.
- Brittain, H. G.; Bogdanowich, S. J.; Bugay, D. E.; Vincentis, J. D.; Lewen, G.; Newman, A. W. Physical characterization of pharmaceutical solid. *Pharm. Res.* **1991**, *8*, 963–973.
- Borka, L. Review on crystal polymorphism of substances in the European pharmacopoeia. *Pharm. Acta Helv.* **1991**, *66*, 16–22.
- Shibata, M.; Kokubo, H.; Morimoto, K.; Morisaka, K.; Ishida, T.; Inoue, M. X-ray structural studies and physicochemical properties of cimetidine polymorphism. *J. Pharm. Sci.* **1983**, *72*, 1436–1442.
- Matsuda, Y.; Kawaguchi, S.; Kobayashi, H.; Nishijo, J. Physicochemical characterization of spray-dried phenylbutazone polymorphs. *J. Pharm. Sci.* **1984**, *73*, 173–179.
- Hirayama, F.; Usami, M.; Kimura, K.; Uekama, K. Crystallization and polymorphic transition behavior of chloramphenicol palmitate in 2-hydroxypropyl- β -cyclodextrin matrix. *Eur. J. Pharm. Sci.* **1997**, *5*, 23–30.

7. Thomas, R. C.; Ikeda, G. J. The metabolic fate of tolbutamide in man and in the rat. *J. Med. Chem.* **1966**, *9*, 507–510.
8. Simmons, D. L.; Ranz, R. J.; Gyanchandani, N. D.; Picotte, P. Polymorphism in pharmaceuticals II (tolbutamide). *Can. J. Pharm. Sci.* **1972**, *7*, 121–123.
9. Burger, A. Zur polymorphie oraler antidiabetika. *Sci. Pharm.* **1975**, *43*, 161–168.
10. Burger, A.; Ramberger, R. On the polymorphism of pharmaceuticals and other molecular crystals. II. Applicability of thermodynamic rules. *Mikrochim. Acta* **1979**, 273–316.
11. Al-Saieq, S. S.; Riley, G. S. Polymorphism in sulphonylurea hypoglycaemic agents: I. Tolbutamide. *Pharm. Acta Helv.* **1981**, *56*, 125–129.
12. Leary, J. R.; Ross, S. D.; Thomas, M. J. K. On characterization of the polymorphs of tolbutamide. *Pharm. Weekblad. Sci. Ed.* **1981**, *3*, 62–66.
13. Umeda, T.; Ohnishi, N.; Yokoyama, T.; Kuroda, T.; Kita, Y.; Kuroda, K.; Tatsumi, E.; Matsuda, Y. A kinetic study on the isothermal transition of polymorphic forms of tolbutamide and mefenamic acid in the solid state at high temperatures. *Chem. Pharm. Bull.* **1985**, *33*, 2073–2078.
14. Traue, J.; Kala, H.; Köhler, M.; Wenzel, U.; Wiegeleben, A.; Förster, B.; Pollandt, P.; Pintye-Hódi, K.; Szabó-Révész, P.; Selmeczi, B. Untersuchungen zur polymorphie von arzneistoffen in pulvern und tabletten. *Pharmazie* **1987**, *42*, 240–241.
15. Georganakis, M. Untersuchungen zur polymorphie von tolbutamid. *Pharmazie* **1989**, *44*, 209–210.
16. Olives, A. I.; Martin, M. A.; del Castillo, B.; Barba, C. Influence of the presence of trace amounts of metals on the polymorphism of tolbutamide. *Int. J. Pharm.* **1996**, *14*, 1069–1076.
17. Stephenson, G. A.; Pfeiffer, R. R.; Byrn, S. R. Solid-state investigation of the tautomerism of acetoexamide. *Int. J. Pharm.* **1997**, *146*, 93–99.
18. *The Japanese Pharmacopeia XIII*; Japanese Pharmacopeial Conversion, Inc.: Tokyo, 1996; pp 116–121.
19. *teXsan: Single-Crystal Structure Analysis Package*, Version 1.6 (1993), Molecular Structure Corporation: The Woodlands, TX.
20. Ueda, H.; Nagai, T. Solid-state nuclear magnetic resonance spectroscopy and Raman spectroscopy of inclusion compound of tolbutamide with β -cyclodextrin. *Chem. Pharm. Bull.* **1981**, *28*, 1415–1421.
21. Carr, D. S.; Hariss, B. L. Solutions for maintaining constant relative humidity. *Ind. Eng. Chem.* **1949**, *41*, 2014–2015.
22. Nyqvist, H. Saturated salt solutions for maintaining specified relative humidities. *Int. J. Pharm. Technol. Prod. Mfr.* **1983**, *4*, 47–48.
23. Nogami, H.; Nagai, T.; Yotsuyanagi, Y. Dissolution phenomena of organic medicinals involving simultaneous phase changes. *Chem. Pharm. Bull.* **1969**, *17*, 499–509.
24. Donaldson, J. D.; Leary, J. R.; Ross, S. D.; Thomas, M. J. K. The structure of the orthorhombic form of tolbutamide (1-*n*-butyl-3-*p*-toluenesulphonylurea). *Acta Crystallogr.* **1981**, *B27*, 2245–2248.
25. Rowe, E. L.; Anderson, B. D. Thermodynamic studies of tolbutamide polymorphs. *J. Pharm. Sci.* **1984**, *73*, 1673–1675.
26. Kimura, K.; Hirayama, F.; Arima, H.; Uekama, K. in preparation.
27. Hancock, J. D.; Sharp, J. H. Method of comparing solid-state kinetic data and its application to the decomposition of kaolinite, brucite, and BaCO₃. *J. Am. Ceram. Soc.* **1972**, *55*, 74–77.

JS980376Z